Erratum: Chiral discrimination in helicity-preserving Fabry-Pérot cavities [Phys. Rev. A 107, L021501 (2023)]

L. Mauro, J. Fregoni, J. Feist, and R. Avriller

(Received 21 July 2023; published 15 December 2023)

DOI: 10.1103/PhysRevA.108.069902

We have found erroneous input parameters both in the captions and in generating the plots of Figs. 2 and 4 of the original paper. The corrected parameters are: a molecular Pasteur layer thickness of 130 nm in both figures, and metallic mirrors of 16 nm thickness in Fig. 2(a). All the other parameters of the published version, summarized in Tables I and II of the supplemental material, remain unchanged. We also found a discrepancy in the implementation of the numerical code used to generate Figs. 2 and 4, for which the erroneous dispersion relation written in Eq. (1) of the supplemental material was used, instead of the correct relation given by $n_{\pm}(\omega) = n(\omega) \pm \kappa(\omega)$. This discrepancy does not affect Eqs. (2)–(7) in the supplemental material, nor the analytical approaches used in the original paper, which remain correct. We provide in this Erratum the proper Figs. 2 and 4, with the correct input parameters and the correct implementation of the dispersion relations in the numerical code. We show two cases (i) a constant and real $\kappa(\omega) \equiv \kappa_0 = -10^{-3}$ corresponding to the original paper, and (ii) a complex and frequency-dependent $\kappa(\omega) = \kappa_0 \frac{\omega \omega_p^2 f}{\omega_0(\omega_0^2 - \omega^2 - i\gamma\omega)}$ with $\kappa_0 = -10^{-3}$, corresponding to Eq. (44) in the supplemental material. Both cases are physically possible but correspond to different Pasteur media.

In case (i), the corrected Fig. 2 (see Fig. 1 below) remains qualitatively unchanged compared to Fig. 2 in the original paper. We remark, however, on the slight quantitative differences in Fig. 2(a) with broader polaritonic peaks due to lower reflectivity of the mirrors, as well as higher polaritonic peaks in Fig. 2(d). Some differences are also seen in Figs. 2(b) and 2(c), leading to a shift of the Fano resonance in Fig. 2(e) from 2 eV towards a lower value ≈1.975 eV. The corrected Fig. 4 is shown below in Fig. 2. We see that in the case of the helicity-preserving cavity, the new Figs. 4(a) and 4(b) remain qualitatively the same compared to the original paper, with the same order of magnitude and line shapes for the computed ΔDCT signals. However, the case of normal mirrors in the new Fig. 4(c) is strongly modified compared to the original paper, and it exhibits a vanishing of the ΔDCT_N signal. This difference is due to two facts: First, with the corrected implementation of the dispersion relation, for real $\kappa(\omega) \equiv \kappa_0$, the medium does not create circular dichroism; and second, the remaining effects of optical activity cancel out, due to polarization-reversal of the propagating electromagnetic waves upon reflection at each medium-mirror interface. In this sense, the helicity-preserving cavity generates an infinite enhancement of ΔDCT since its transmission is sensitive to the optical activity of the medium, in contrast to a conventional Fabry-Pérot cavity.

For completeness, we show how Fig. 4 is modified in case (ii) of complex $\kappa(\omega)$. In this case, for normal mirrors, the circular dichroism does not vanish anymore, and ΔDCT_N scales with ω_p^2 [see Fig. 3(c)]. For helicity-preserving cavities [see Fig. 3(b)], the obtained ΔDCT signal changes significantly compared to Fig. 2(b). We also note that in this case, there is no significant enhancement of ΔDCT compared to ΔDCT_N, both signals being of order κ_0. Varying the length of the Pasteur layer to

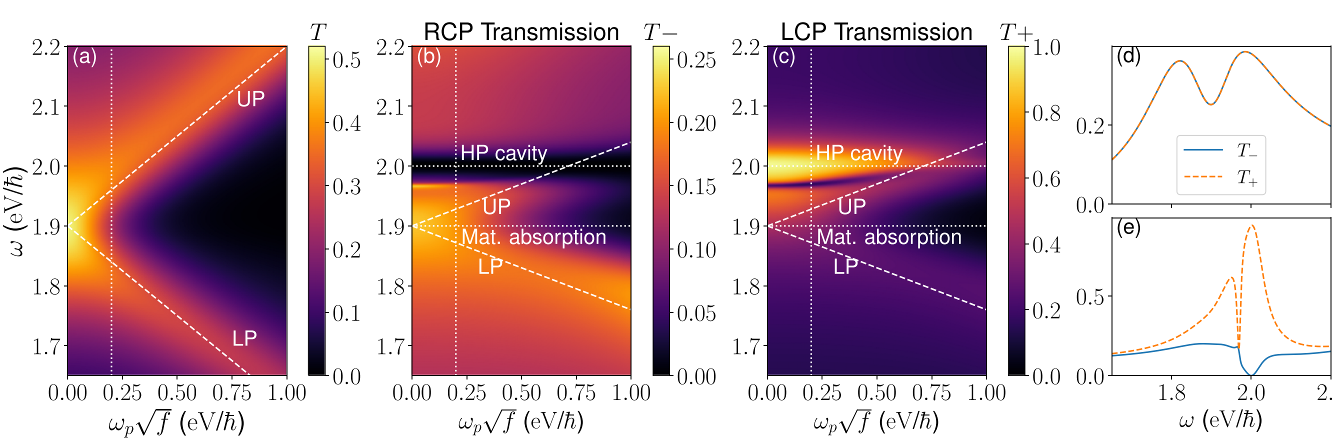

FIG. 1. Corrected Fig. 2 corresponding to the original paper.

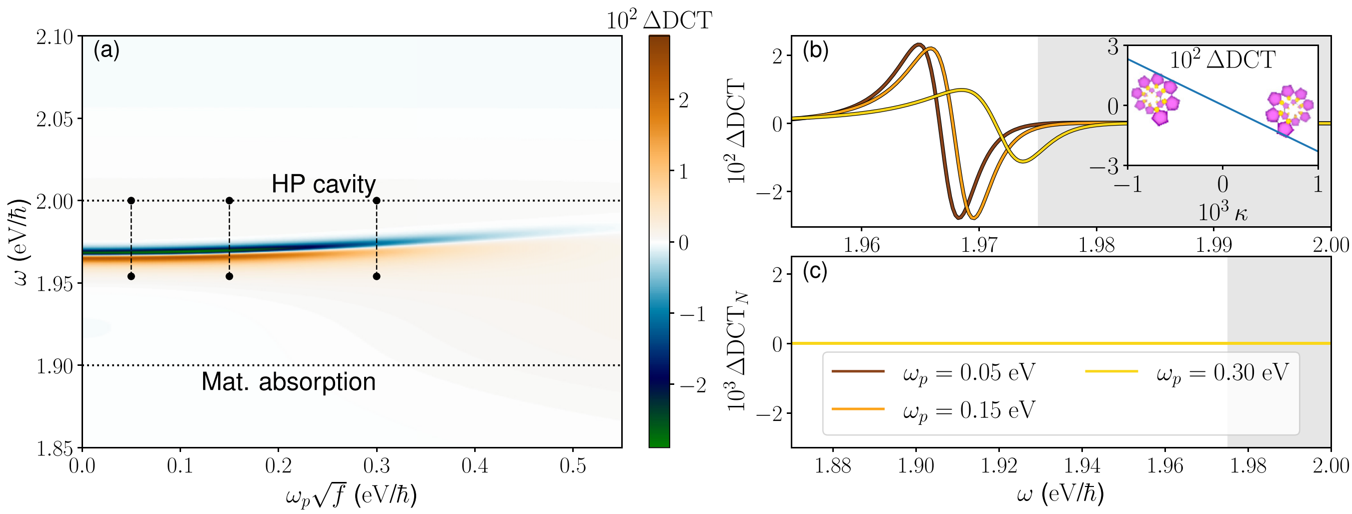

FIG. 2. Corrected Fig. 4 corresponding to the original paper.

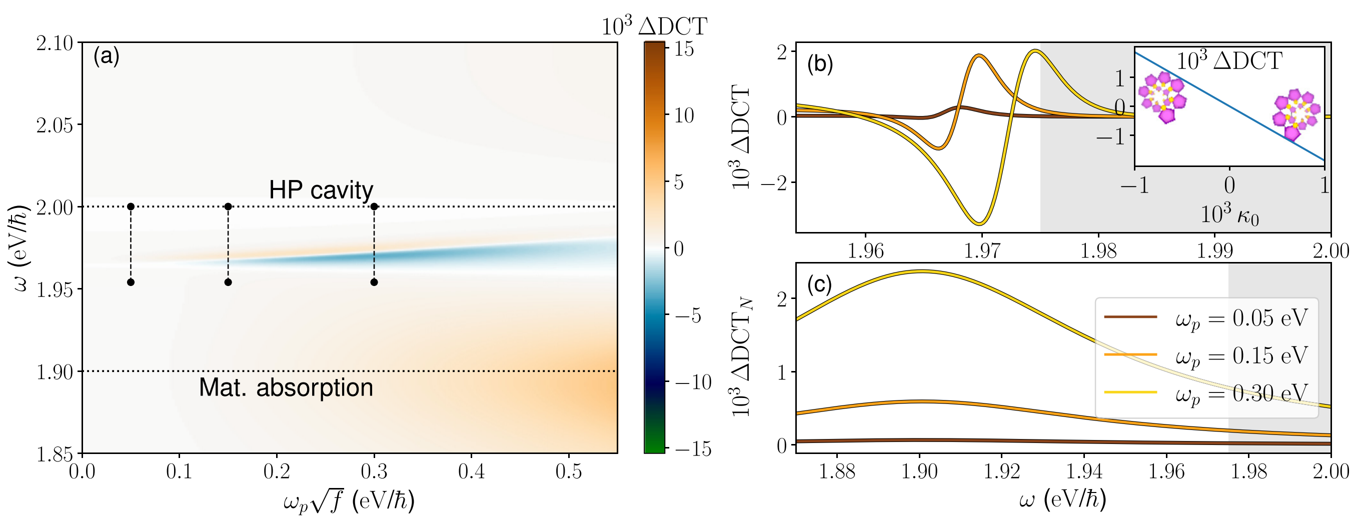

FIG. 3. Figure 4 in the new case (ii) of $\kappa(\omega) = \kappa_0 \frac{\omega\omega_p^2 f}{\omega_0(\omega_0^2-\omega^2-i\gamma\omega)}$ for $L = 130$ nm. The inset is computed for $\omega = 1.97$ eV/$\hbar$ and $\omega_p\sqrt{f} = 0.15$ eV/$\hbar$.

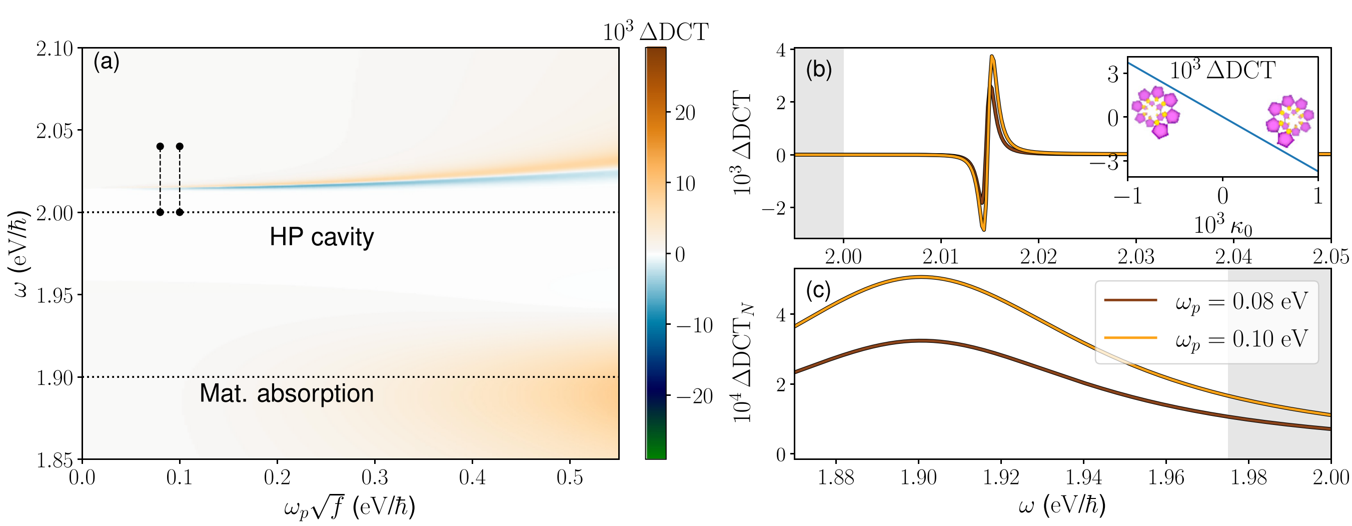

FIG. 4. Figure 4 in the new case (ii) of $\kappa(\omega) = \kappa_0 \frac{\omega\omega_p^2 f}{\omega_0(\omega_0^2-\omega^2-i\gamma\omega)}$, $L = 250$ nm. The inset is computed for $\omega = 2.015$ eV/$\hbar$ and $\omega_p\sqrt{f} = 0.1$ eV/$\hbar$.

$L = 250$ nm, we were nevertheless able to find a range of parameters for which an enhancement of the chiroptical response by one order of magnitude is seen [see Fig. 4(b) versus Fig. 4(c) below], although this occurs in a narrow range of frequencies.

The main conclusion of our paper thus holds, namely that we found a model of a helicity-preserving Fabry-Pérot cavity predicting a large sensitivity in chiral-sensing measurements, while the use of normal mirrors in the same conditions would lead to a weak (here vanishing) sensitivity. However, we have to clarify and complement this statement: with our model in the original paper, the ΔDCT chiroptical signals are actually generated by mirror-induced optical activity and not by circular dichroism. We have shown in this Erratum a different parametrization of the Pasteur coefficient for which both optical activity and circular dichroism contribute to ΔDCT. In this latter case, sensitivity enhancement is harder to achieve, because it results from an interference process between the designed chiral mirrors and the Pasteur material chiroptical properties. Whether measuring ΔDCT with such a helicity-preserving cavity would be advantageous compared to the measurement of optical rotation will depend on the details of the experimental setup. We hope that our results will stimulate further experimental works along this direction.